Revista Ciencia en Desarrollo. Vol. 16 Num. 2. pp. 210 - 221
julio - diciembre

DOI: 10.19053/uptc.01217488.v16.n2.2025.19052

Artículo de investigación

Sustainable purification of biodiesel from waste frying oils using coffee biomass

Purificación sostenible de biodiésel a partir de aceites de fritura usados utilizando biomasa de café

Enna Rocio Mejía-Silva[1]✉, Jaime Fernando Martínez-Suárez[2]✉ and Nasly Delgado[3]✉

[1]Grupo de investigación SIMABID, Facultad de Ciencias Básicas, Universidad de la Amazonia, Florencia, Colombia.
[2]Programa de Química, Facultad de Ciencias Básicas, Universidad de la Amazonia, Florencia, Colombia.
[3]Grupo de Ciencia e Ingeniería en Sistemas Ambientales, Departamento de Ingeniería Ambiental, Facultad de Ingeniería Civil, Universidad del Cauca, Popayán, Colombia.

Recepción: 26-marzo-2025 **Aceptado:** 07-junio-2025 **Publicado:** 20-julio-2025
Cómo citar: Mejía-silva, E. R., Martínez Suárez, J. F., & Delgado, N. (2025). Purificación sostenible de biodiésel a partir de aceites de fritura usados utilizando biomasa de café. *Ciencia En Desarrollo*, 16(2). doi: 10.19053/uptc.01217488.v16.n2.2025.19052

Abstract

In recent decades, rapid population growth and the increasing need to meet energy demands have led to implementing alternative fuels derived from common waste materials. One such example is biodiesel, which can be produced from used cooking oil. Among the various stages involved in the production of biodiesel, the purification process is of significant concern due to its considerable environmental impact, primarily because of the large volumes of water used. Non-conventional purification methods, such as dry washing, are being explored as promising alternatives. However, the adsorbent material employed in these processes must ensure the effective removal of contaminants, thus ensuring that the resulting biodiesel meets international standards. Hence, the utilization of a byproduct from the coffee industry, namely coffee husk, was examined for its conversion into activated carbon. The husk underwent physical activation at temperatures ranging from 600 to 800 ºC for durations of 30 and 90 min. Additionally, chemical activation was employed using H_3PO_4 at concentrations ranging from 50% to 85% and KOH ratios ranging from 1:1 to 1:3. A free glycerol concentration in the biodiesel sample of 0.17% w/w was measured. The activated carbon produced using KOH at a concentration of 1:1 exhibited the most effective glycerol removal properties, achieving a concentration of 0.020% w/w within a contact time of 2.5 h. Regarding the characteristics of the adsorbent material, it exhibited a specific surface area of 1412.31 m^2/g, a total pore volume of 0.64 cm^3/g, and an average pore diameter of 1.8 nm. The maximum free glycerol adsorption capacity was determined to be 5.78 ± 0.03 mg/g, fitting well with the Langmuir isotherm. Additionally, the data were fitted to the pseudo-first-order model, yielding kinetic constants ranging from 0.289±0.004 to 0.632±0.003 for material concentrations ranging from 0.1% to 3.0%. Hence, it can be inferred that dry purification with activated carbon derived from coffee husks presents an appealing alternative for biodiesel treatment, facilitating compliance with quality standards. The utilization of such alternatives, sourced from industrial waste, not only adds economic value but also aligns with sustainable development goals.

Keywords: Adsorption isotherms, adsorption kinetics, agro-industrial waste, removal efficiency, physico-chemical activation.

Resumen

En las últimas décadas, el rápido crecimiento de la población y la creciente necesidad de satisfacer la demanda energética han llevado a implantar combustibles alternativos derivados de materiales de desecho comunes. Un ejemplo de ello es el biodiésel, que puede producirse a partir de aceite de cocina usado. Entre las diversas etapas que intervienen en la producción de biodiésel, el proceso de purificación es motivo de gran preocupación debido a su considerable impacto ambiental, principalmente por los grandes volúmenes de agua utilizados. Se están explorando métodos de purificación no convencionales, como el lavado en seco, como alternativas prometedoras. Sin embargo, el material adsorbente empleado en estos procesos debe garantizar la eliminación eficaz de los contaminantes, asegurando así que el biodiésel resultante cumpla las normas internacionales. Por ello, se examinó la utilización de un subproducto de la industria cafetera, la cáscara de café, para su conversión en carbón activado. La cáscara se sometió a activación física a temperaturas comprendidas entre 600 y 800 °C durante períodos de 30 y 90 min. Además, se empleó la activación química utilizando H_3PO_4 en concentraciones que oscilaron entre el 50 % y el 85 % y proporciones de KOH que oscilaron entre 1:1 y 1:3. Se midió una concentración de glicerol libre en la muestra de biodiésel de 0,17% p/p. El carbón activado producido utilizando KOH a una concentración de 1:1 mostró las propiedades de eliminación de glicerol más eficaces, alcanzando una concentración de 0.020% p/p en un tiempo de contacto de 2.5 h. En cuanto a las características del material adsorbente, exhibió una superficie específica de 1412.31 m^2/g, un volumen total de poros de 0.64 cm^3/g, y un diámetro medio de poros de 1.8 nm. Se determinó que la capacidad máxima de adsorción de glicerol libre era de 5.78 ± 0.03 mg/g, ajustándose bien a la isoterma de Langmuir. Además, los datos se ajustaron al modelo de pseudo-primer orden, obteniéndose constantes cinéticas que oscilaban entre 0.289 ± 0,004 y 0.632 ± 0.003 para concentraciones de material entre 0.10 % y 3.0 %. Por lo tanto, se puede inferir que la purificación en seco con carbón activado derivado de cáscaras de café presenta una alternativa atractiva para el tratamiento de biodiesel, facilitando el cumplimiento de las normas de calidad. La utilización de este tipo de alternativas, procedentes de residuos industriales, no sólo añade valor económico, sino que también se alinea con los objetivos de desarrollo sostenible.

Palabras Clave: Matriz biopolimérica, liberación de herbicidas, encapsulación, organobentonita, formulación de liberación lenta, voltamperometría cíclica, electrodo de cobre.

E-ISSN: 2462-7658

1 Introduction

One of humanity's greatest challenges is to address climate change, leading to the adoption of various international mechanisms aimed at mitigating greenhouse gas (GHG) emissions, particularly within one of the fastest growing and most crucial sectors: transportation [1]. In this context, biofuels like biodiesel emerge as an appealing environmental alternative. They are easily degradable, and when blended with diesel, they enhance the lubricity of fossil fuels, consequently reducing wear on vehicle engines [2]; emissions of soot, sulfur, and carbon dioxide are also diminished, thereby mitigating dependence on fossil fuels for energy [3]. The main large-scale challenge in using biodiesel compared to petroleum diesel is the high cost of raw materials. As an alternative to address this dependency, The use of waste frying oil (WFO) is crucial. WFO is a common waste in households, restaurants, and industries, often improperly disposed of by being discharged into water bodies. This affects not only water quality but also human health and the environment [3-7]. There are different methods for producing biodiesel, including pyrolysis, micro-emulsion, dilution, and transesterification [8]. The most widely used process for biodiesel production is transesterification. This process involves three consecutive reversible reactions in which vegetable oil (triglycerides) and short-chain alcohol (primarily methanol or ethanol) react in the presence of an alkaline catalyst, such as ion exchange resins, as well as supercritical fluids and reaction media. The outcome of these reactions is the production of alkyl esters and glycerin [9]. Each reaction yields one ester molecule, resulting in a total of three ester molecules and one glycerol for every triglyceride molecule [10]. This process offers advantages such as lower cost and reduced production time.

After transesterification, the products need to be separated. However, the chemical and physical properties of WFO differ from those of fresh refined vegetable oils. This distinction arises from alterations during the frying process, as WFO undergoes chemical reactions such as hydrolysis, oxidation, and polymerization due to contact with food [11]. The presence of free fatty acids may reduce the reaction yield (formation of methyl esters), thereby promoting soap formation during biodiesel production [12]. For this reason, purification processes involve successive washes to eliminate soap, traces of free glycerine, glycerides, salts, and methanol, which are common contaminants in industrial biodiesel production [11], implying an increase in the total cost of production [2]. Moreover, this traditional washing process requires large volumes of water, raising environmental and operational concerns. In contrast, dry washing with adsorbents emerges as a highly relevant alternative for the industry, as it enables the efficient removal of impurities without excessive water consumption, thereby enhancing the sustainability and feasibility of the process. Therefore, alternatives, such as dry washing using activated carbon adsorbents, have been explored for the removal of these impurities [13, 14, 15]. Few studies have focused on the field of biodiesel purification despite the wide range of applications of activated carbon in solutions for the removal of various pollutants [16, 17, 18]. Therefore, this study evaluates the use of coffee husks, a low-cost, abundant, and renewable agro-industrial waste from coffee cultivation, as an alternative for generating adsorbent materials. This husk is rich in organic compounds, primarily cellulose, hemicellulose, and lignin, which, after a carbonization process, promote the formation of a porous carbonaceous structure ideal for contaminant adsorption. Additionally, it contains oxygen and hydrogen, which facilitate the generation of oxygenated functional groups. It is important to highlight that Colombia is one of the world's leading coffee producers; however, coffee husk residues are not yet integrated into its value chain and are mostly discarded, causing a negative environmental impact. This study proposes utilizing these residues as raw material to produce activated carbon, which will be employed in a dry-washing process for the removal of contaminants, such as free glycerin, from biodiesel obtained from WFO. Additionally, it's noteworthy that there is a lack of comprehensive experimental data on the characterization, behavior, and mathematical modeling of this type of adsorbent. Therefore, beyond obtaining and characterizing diverse adsorbent materials derived from coffee husks, this research delves into studying their equilibrium and adsorption kinetics. Importantly, the utilization of industrial waste in both the biodiesel production and purification processes underscores the potential of this research to contribute significantly to sustainable development.

2 Methodology

2.1 Characterization of waste frying oil and biodiesel production

Waste frying oil (WFO) from the gastronomic school of Tecnoparque Yamboró (Pitalito, Colombia) was used to produce biodiesel. Physicochemical characterization of WFO included measurements of acid index, density, viscosity, free glycerol, and volatile matter [19]. To produce biodiesel, 500 g WFO + 1.0 % KOH/methanol (ratio 1:6) was heated at 60 °C for 2.0 h [20]. At the end of the reaction, the mixture was transferred to a reparatory funnel for 24 h, and the biodiesel was stored for further purification.

2.2 Determination of free glycerol

The quantification of free glycerol in the biodiesel samples was determined by UV-Vis spectrophotometry using a two-step reaction process. The sample is first treated with sodium periodate. Sodium periodate reacts with free glycerol in the sample to generate formaldehyde. The reaction between this formaldehyde and acetylacetone produces the yellow complex, 3.5-diacetyl-1.4-dihydrolutidine. This yellow compound exhibits a maximum absorbance peak at 410 nm, where free glycerol concentration in the sample is measured [21]. A reference solution of 0.036 mg/mL glycerol in a 1:1 mixture of deionized water and 95 % ethanol (working solution) was used for the calibration curve in a concentration range of 0.38 to 3.0 % w/w. For the biodiesel sample, 1.0 g sample was weighed and dissolved in 4.0 mL hexane + 4.0 mL working solution, then shaken for 5.0 min and centrifuged for 15 min at 2000 rpm. After centrifugation, the top layer was removed with a Pasteur pipette. Each standard and the sample (0.50 mL) were treated with 1.2 mL of a 10 mM sodium periodate solution and shaken for 30 seconds. Each solution was then treated with 1.2 mL of a 0.20 M acetylacetone solution, placed in a water bath at 70 °C for 1.0 minute, and stirred. The solutions were immediately placed in cold water to stop the reaction. Standards and samples were measured at 410 nm [22].

2.3 Production of adsorbent materials

The biomass used in the preparation of the activated carbon consisted of production residues from coffee agro-industry roasting (husk). The husks underwent manual removal of impurities and were then dried at 100 °C for 72 h. Activation was achieved through both physical and chemical processes. In the physical activation process, the sample was activated at temperatures from 600 to 800 °C, with varying time intervals between 30 and 90 min. Subsequently, the material was macerated and sieved through a mesh with a diameter of 106 μm [23, 24, 25].

In the chemical activation process, the carbonized samples were utilized, to which KOH was added with ratios of carbon mass/activation agent of 1:1 and 3:1 [25]. The sample was heated to a temperature of 800 °C for 30 min. Subsequently, distilled water at 90 °C was added. After shaking and filtration, a 0.1 M HCl solution was introduced until the sample was immersed. Subsequently, sonication for 1.0 h was employed for homogenization, followed by another round of vacuum filtration. The sample underwent a wash with distilled water at 90 °C and an immediate rinse with 0.10 M HCl until achieving a pH between 6.0-7.0 units. Finally, the sample was filtered and subjected to heating at 100 °C for 12 h.

Chemical activation was assessed by immersing the carbonized sample in 50% and 85% H_3PO_4 solutions [26]. The sample was then sonicated for 2.0 h to ensure homogenization. Subsequently, it was heated to 120°C for 24 h, followed by exposure to 800 °C for

1.0 h. After cooling to 22°C, the sample was washed with distilled water, filtered under vacuum, and rinsed with 0.10 M NaOH while continuously agitating for 30 min. It was then filtered again and washed with distilled water until reaching a pH of 6.0-7.0. Finally, the sample was filtered once more and incubated at 110°C for 24 h.

2.4 Characterization of adsorbent materials

NIR spectra were recorded using a SpectraStar™ model 400 XL spectrophotometer in the wavelength range 680 to 2600 nm. Absorption spectra were obtained using a UV-vis spectrophotometer (Shimadzu UV-1800). The morphological structures were analyzed by scanning electron microscope (SEM) in a Carl Zeiss (model EVO HD 15). The Brunauer–Emmett–Teller surface areas (BET) were collected by N_2 adsorption isotherm using a Micromeritics 3 Flex analyzer at 77 K. Electrochemical measurements were performed on a 797 VA Computrace potentiostat/galvanostat (Metrohm). The cell contained a glass carbon (GC) working electrode, a platinum auxiliary electrode, and an Ag|AgCl|KCl (3.0 M) double junction reference electrode. The GC electrode was modified by drop-casting; 5.0 μL of the suspension (5.0 mg of activated carbon + 5.0 mL of type I water were placed in an ultrasonic bath for 30 min) was placed on the GC electrode and dried at 50 °C for 10 min.

2.5 Adsorption of free glycerol on activated carbon

Initially, adsorption profiles were evaluated to determine the appropriate material for free glycerol removal. In these preliminary studies, a concentration of 1.1 % w/w of each activated carbon obtained from the biodiesel sample was brought into contact, which had a density of 879 kg/m^3. The samples were analyzed in triplicate, maintaining constant agitation and temperature at 120 rpm and 26 °C, respectively, and eight sampling times between 0.50 to 24 h were examined. Aliquots of 2.0 mL were taken at each time point, centrifuged at 2000 rpm for 15 min, and the supernatant was analyzed using UV-Vis spectrophotometry at a wavelength of 410 nm. Subsequently, the effect of adsorbent loading on free glycerol removal was studied, evaluating concentrations of (0.10, 0.25, 0.50, 1.0, 2.0, and 3.0) % w/w of activated carbon in biodiesel and contact times between 1.0 and 5.0 h, under the same testing conditions.

2.6 Equilibrium and adsorption kinetics studies

The equilibrium adsorption experiments were conducted in triplicate, varying the concentrations of activated carbon in biodiesel from 0.10 to 3.0 % w/w, at 120 rpm and 26 °C for 2.5 h. Langmuir, Freundlich, Langmuir-Freundlich combined isotherm, and Redlich-Peterson models were employed to elucidate the mechanism of free glycerol adsorption onto the adsorbent, determining its adsorption capacity and its influence on the adsorption process. Kinetic studies were performed using the same concentrations, agitation, and temperature as in the equilibrium experiments. However, in this case, samples were taken at different time points (0.0, 1.0, 1.5, 2.5, 3.0, 4.0, and 5.0) h. The obtained values were analyzed using the pseudo-first-order kinetic model and the pseudo-second-order kinetic model.

2.7 Biodiesel purification

The purification of biodiesel was carried out using both conventional and dry washing methods. Conventional purification involved water washing using a separating funnel at a biodiesel-water ratio of 3:1. The mixture was then agitated and allowed to settle for 15 min. This process was repeated until the sample reached a pH of approximately 7.0 units. Finally, the biodiesel was dried at 105°C for 24 h [27].

For the dry washing purification, 0.50 % w/v of activated carbon was added to biodiesel under constant agitation and temperature of 120 rpm and 26 °C, respectively. The mixture was then filtered under a vacuum. Physicochemical characteristics such as acidity index, density, viscosity, moisture, and volatile matter were determined for both conventionally and dry-washed purified samples.

3 Results and discussion

3.1 Characterization of WFO

Biodiesel quality depends on the feedstock and the production process [28]. Also, the physicochemical properties of WFO [29]. Thus, the results obtained for WHO were 0.198 ± 0.007 mg KOH/g (acid number), 879.1 ± 0.8 kg/m^3 (density), 39.7 ± 0.6 mm^2/s (viscosity), 1.61 ± 0.03 % w/w (free glycerol) and 0.042 ± 0.001 mg/kg volatile matter. The acid index measures the content of free fatty acids [30]. For our study, it was 0.19 mg KOH/g WFO, and this value is below < 1.0 mg KOH/g sample, which is recommended for base-catalyzed transesterification [31]. Transesterification is a simple, efficient, low-cost, and short production time procedure, which is why it is widely used in biodiesel production [32].

3.2 Conditions and performance of adsorbent materials

Table 1 describes the conditions under which the activated carbons were obtained and their percentage yield. It is observed that the yield of activated carbons is lower when a temperature of 800°C is used, as higher activation temperatures lead to a faster reaction rate, resulting in more carbon burning and the release of more volatile components [25]. Other studies have reported the production of activated carbon from coffee husks using KOH under conditions like those of the present study, yielding higher efficiencies of 16.5 % for a 1:1 ratio and 14.2 % for a 1:3 ratio. These efficiencies are attributed to working with an inert atmosphere in the presence of N_2 [25], thus indicating the importance of conducting studies while maintaining an inert atmosphere.

Table 1: Activation conditions and yield of activated carbon samples

Activation	Temperature (°C)	Time (min)	Sample	Yield (%)
Physical	600	90	AC-600-90	14.2
Physical	800	30	AC-800-30	13.1
Physical	800	90	AC-800-90	13.3
Chemical (KOH 1:1)	800	90	AC-KOH-1:1	9.10
Chemical (KOH 1:3)	800	90	AC-KOH-1:3	9.40
Chemical (H_3PO_4 50%)	800	90	AC-H_3PO_4-50%	6.80
Chemical (H_3PO_4 85%)	800	90	AC-H_3PO_4-85%	6.90

3.3 Characterization of adsorbent materials

3.3.1 Optical properties

NIR spectra are difficult to distinguish differences in activated carbons due to overtones and combinations from the primary absorption in the mid-infrared region with many overlapping peaks and valleys [33]. Figure 1A shows the NIR spectra of activated carbons in the 1000-2300 nm spectral region. All spectra are similar in appearance, with an assignment of bands at 1337 and 1350 (C-H), 1410 (C-H and ArOH), 1930 (R-CO_2-R), 1975 (CONH), 2200 (CHO), 2330 and 2510 (CH + C-C) nm [34, 35]. The main difference between the samples is absorbance intensities; for host materials activated by a chemical process, no changes in absorption band intensities were observed. However, with physically activated carbons, higher absorbance intensity at 1337 and 1350 nm is observed with increasing temperature and time due to higher carbon content and darker sample color [36].

Figure 1B shows the UV-Vis spectra of activated carbons measured from the same suspensions used in the electrochemical analysis in the 200-1100 nm absorbance range. All activated carbon samples show two absorption maxima around 750 and 970 nm in the NIR region, characteristic of the antisymmetric O-H stretching and third overtone of the O-H bonds in water, respectively [37, 38]. A broad

absorption peak around 260 nm was observed for the chemically activated carbons and is related to the electronic transitions between the π - π^* orbitals in the carbonaceous materials [39, 40]. However, this signal was not observed in the physically activated carbons, indicating a higher molecular weight and aromaticity in the carbon structure [41, 42, 43].

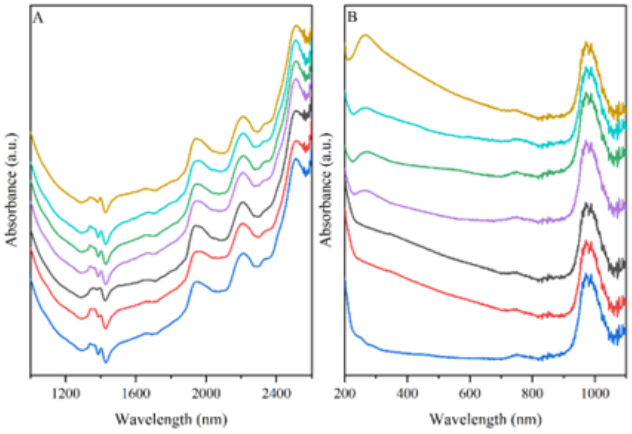

Figure 1: Figure 1. A) NIR and B) UV–Vis spectra for activated carbons: AC-600-90 (—), AC-800-30 (—), AC-800-90 (—), AC-H_3PO_4-85% (—), AC-H_3PO_4-50% (—), AC-KOH-1:1 (—), AC-KOH-1:3 (—).

3.3.2 Electrochemical analysis

The electrochemical characterization of the activated carbons was carried out by cyclic voltammetry (CV). CV can rapidly provide information on the thermodynamics of redox processes, kinetics of heterogeneous electron transfer reactions, and coupled chemical reactions or adsorption processes [44]. Therefore, there are correlations between adsorption processes and the electrical properties of activated carbon electrodes [45, 46]. Thus, activated carbon samples with a high specific surface area (SSA) have a high electrical conductivity because a high SSA increases the mobility of ions/molecules within the material's pores [47]. Figure 2 shows the VCs of activated carbon evaluated against a 50 mM $Fe(CN)_6^{3-/4-}$ (1:1 mol ratio) + 0.10 M KCl solution. The CVs were analyzed by comparing the electrochemical response of the GC electrode concerning its modification with the activated carbon suspension under different conditions. The VCs for carbon activated by physical processes (Figure 2A) show a lower reversibility of the redox process to chemical activation (Figure 2B and 2C), indicating a higher resistance to the charge transfer of the redox process (lower electrical conductivity). However, a change in temperature to 800 °C, and the application time (30 and 90 min) for the physical activation of the carbon for the pristine sample (600 °C and 30 min), causes an improvement in the reversibility of the electrochemical response of the redox couple (Figure 2A). On the other hand, basic chemical activation (Figure 2B) shows higher peak currents related to acid chemical activation (Figure 2C), indicating an increase in the electroactive area of the GC electrode (higher electrical conductivity) [48].

3.3.3 SEM analysis

SEM analyzed the morphological study of the activated carbons. The arithmetic means roughness (Ra), average pore distribution, and pore number were measured using the ImageJ software [49]. Surface topography affects the adsorption of substances of interest [50, 51, 52]. Figures 3A and 3E show the heterogeneous particle size and a rough surface (Figures 3B and 3G) on the activated carbons. Also, Ra values for the activated carbons were higher than 10 μm, indicating a high roughness (Figure 3F). AC-H_3PO_4-85 % activated sample showed 20 % higher roughness (Ra value) than KOH or physical activation. Thus, as the roughness increases, the surface area increases, but roughness can also change the chemical homogeneity of the surface [53]. On the other hand, AC-800-90, AC-H_3PO_4-50 %, and AC-KOH- 1:3 samples show pores on the surface (Figure 3C, 3D and 3H). Figure 3I shows the average pore distribution and pore number. Physical activation (2.64 μm) showed a higher pore size distribution than KOH (0.77 μm) or H_3PO_4 (2.17 μm) activation, but a lower pore number was observed. AC-KOH-1:3 sample presented the best pore number to pore size ratio, which can improve the adsorption of organic compounds.

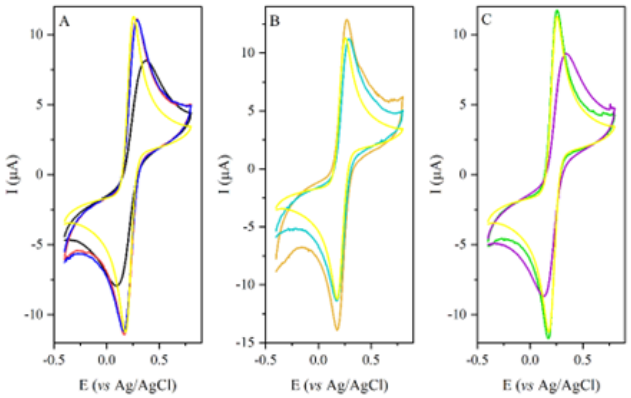

Figure 2: CVs for activated carbons. A) AC-600-90 (—), AC-800-30 (—), and AC-800-90 (—). B) AC-KOH-1:1 (—) and AC-KOH-1:3 (—). C) AC-H_3PO_4-85% (—) and AC-H_3PO_4-50% (—). Scan rate 100 mV s^{-1}. GC electrode.

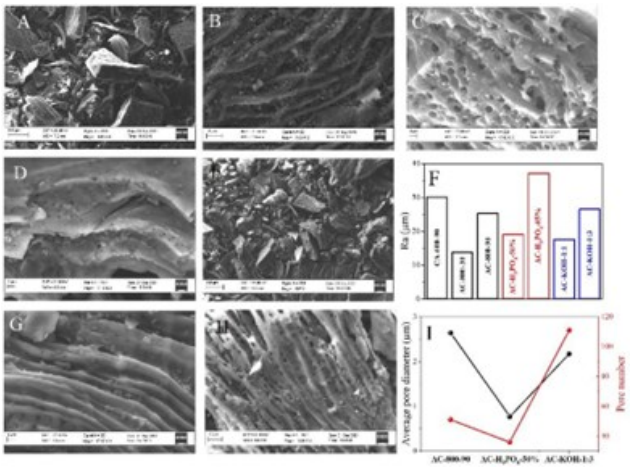

Figure 3: SEM for activated carbons: A) AC-600-90, B) AC-800-30, C) AC-800-90, D) AC- H_3PO_4-50%, E) AC- H_3PO_4-85%, G) AC-KOH-1:1 and H) AC-KOH-1:3. F) Arithmetic mean roughness (Ra). I) Average pore distribution and pore number.

3.4 Adsorbent material effect on free glycerol removal

Initially, the adsorption profiles of free glycerol onto different adsorbent materials over time were studied, as depicted in Figure 4A. An initial glycerol concentration of 0.16 ± 0.05 % w/w was obtained for crude biodiesel. According to the results obtained, it was determined that equilibrium was reached at 2.0 h with the AC-KOH-1:1 and AC-KOH-1:3 carbons, achieving removal rates exceeding those established by international standards (ISO 14214-1:

maximum limit 0.02% w/w). However, the other materials did not meet the permissible maximum limit of glycerol in biodiesel. No statistically significant differences (p-value = 0.11) were found between the treatments of AC-KOH-1:1 and AC-KOH-1:3 according to the Kruskal-Wallis one-way analysis and Shapiro-Wilks test ($p \leq 0.05$). Therefore, it is concluded that the most suitable material for glycerol removal is AC-KOH-1:1.

Afterward, the effect of the mass of AC-KOH-1:1 carbon on free glycerol removal was evaluated. According to the results shown in Figure 4B, it was determined that increasing the mass of carbon, in concentrations ranging from 0.50 to 3.0%, achieves high removal rates of free glycerol within a contact time of 2.5 h, reaching equilibrium at concentrations of 0.002% w/w, complying with the permissible maximum limits set by standards (ISO 14214-1: 0.02% w/w). No statistically significant differences were found between carbon concentrations of 0.50 %, 1.0 %, 2.0 %, and 3.0 %, as indicated by a p-value of 0.063 from the Kruskal-Wallis one-way analysis and Shapiro-Wilks test ($p \leq 0.05$). Thus, it was concluded that the optimal mass of AC-KOH-1:1 was 0.50 g. These data on the type of material to use, its optimal loading, and contact time allow us to define the initial design parameters to scale up this system, and even the sizing of adsorption columns, following designs reported in the literature for adsorption processes of contaminants in aqueous solutions.

The removal of free glycerol in biodiesel has been evaluated using materials such as sugarcane bagasse, where minimum loads of the adsorbent material of 2.0 % w/w are reported to meet standards, which is higher than that obtained in the present research [54, 55]. Similarly, materials from rice husks have been used, where no significant differences were found when using adsorbent loads between 1 to 5.0 % w/w to comply with standards, which is like the efficiencies found in the present study. However, lower ratios that define the optimal working mass were not studied [56]. It is important to note that none of these studies conducted kinetic studies to assess the behavior of the adsorbent over time, as analyzed in the following sections of this study.

On the other hand, a BET analysis was performed on AC-KOH-1:1. Figure 1S (supplementary material), shows the N_2 adsorption curve; this presents an accentuated adsorption in low P/P0 values (P/P_0 0.2), indicating mainly the presence of microporous, with a diameter lower than 2.0 nm. This result agrees with what was observed in the SEM analysis. The activated carbon obtained from coffee husk exhibits a specific surface area of 1412.3 m^2/g, indicating a high availability of active sites for glycerin adsorption. Its pore volume of 0.64 cm^3/g suggests an adequate capacity for contaminant retention, while its average pore diameter of 1.8 nm indicates a predominantly microporous structure. Given that glycerin has an approximate molecular size of 0.9 nm, the material's microporosity favors its adsorption through physical interactions such as Van der Waals forces. However, the limited presence of mesopores could restrict molecular diffusion toward internal sites, affecting the adsorption rate. To optimize the material's efficiency in glycerin removal, it would be advisable to evaluate structural modifications that increase the proportion of mesopores. Additionally, to better characterize its performance under real adsorption conditions, kinetic and isothermal studies were assessed in the following sections. Similar results were obtained for a coffee husk-activated carbon in a basic medium as an adsorbent for dehumidification [57].

3.5 Adsorption isotherms

The Langmuir and Freundlich isotherms were analyzed using two-parameter models. In contrast, the combined Langmuir-Freundlich and Redlich-Peterson isotherms were analyzed with three-parameter models to study the adsorption equilibrium. Nonlinear regression models were employed to better capture the relationship between the data and the evaluated models, describing the parameters under study more accurately. To analyze the adsorption capacity of free glycerol onto AC-KOH-1:1, the interaction of three properties was considered: the concentration of free glycerol on the adsorbent (q_e), the concentration of the adsorbate in aqueous solution (C_e), and the temperature of the system (t). The experiments were conducted at temperature and agitation constant of 26 °C and 120 rpm, respectively, for 2.5 h with a carbon loading of 0.50 %. In this field of research on dry washing for biodiesel purification, to the best of the authors' knowledge, no studies on equilibrium and adsorption kinetics have been reported.

To determine the value of the amount of adsorbed substance over time (q_t) in mg/g, Equation 1 was applied:

$$q_t = \frac{(C_0 - C_t)V}{W} \tag{1}$$

Where C_0 and C_t are the initial and at-time t concentrations (mg/L), V is the volume of solution (L), and W is the amount of adsorbent (g). The fitting for each of the evaluated isotherms is presented in Table 2 and Figure 2S of the supplementary material.

3.5.1 Langmuir isotherm

The Langmuir model assumes the existence of identical and energetically equivalent sites on a homogeneous surface, where an equal number of molecules are transported per site without interaction between the adsorbate molecules [58]. This is described by Equation 2:

The Langmuir model assumes the existence of identical and energetically equivalent sites on a homogeneous surface, where an equal number of molecules are transported per site without interaction between the adsorbate molecules [58]. This is described by Equation 2:

$$q_e = \frac{q_m K_L C_e}{1 + K_L C_e} \tag{2}$$

Where q_e is the amount of adsorbate adsorbed per unit mass adsorbent at equilibrium (mg/g), q_m is the maximum adsorption capacity (mg/g), K_L is the adsorption constant (L/mg), and C_e is the adsorbate equilibrium concentration (mg/L). The dimensionless ratio R_L can also be determined to ascertain whether the isotherm is favorable ($0 < R_L < 1$), linear ($R_L = 1$), unfavorable ($R_L > 1$), or irreversible ($R_L = 0$), as proposed in Equation 3 [59]:

$$R_L = \frac{1}{1 + K_L C_o} \tag{3}$$

Table 2 shows the parameters obtained from the adjustment of the nonlinear equation. The correlation coefficient was 0.76 ± 0.01 and the p-value < 0.0001 for a significance level of 0.05. The R_L was calculated for experimental data, yielding a value of 0.04, indicating the applicability of the Langmuir isotherm for these systems. The q_m was 5.78 ± 0.03 mg/g. The obtained result was lower than that reported for adsorption with raw sugarcane bagasse, where a value of 88.9 mg/g was reported [2]. There are no reports on the equilibrium behavior of free glycerol in a biodiesel sample using activated carbon as an adsorbent.

3.5.2 Freundlich isotherm

It is based on multilayer adsorption with adsorption sites of different energies, not necessarily identical and not always available. The mathematical expression of the isotherm is given by Equation 4:

$$q_e = K_F C_e^{1/n} \tag{4}$$

Where, K_F (mg/g) $(L/mg)^{1/n}$ is considered as an equilibrium constant, and n can be associated with the affinity of the adsorbent and the adsorbate. Normally, $1/n < 1$. The value of $1/n < 1$ was 0.29. In Table 2, it is shown that the correlation coefficient value was 0.61 ± 0.00 with

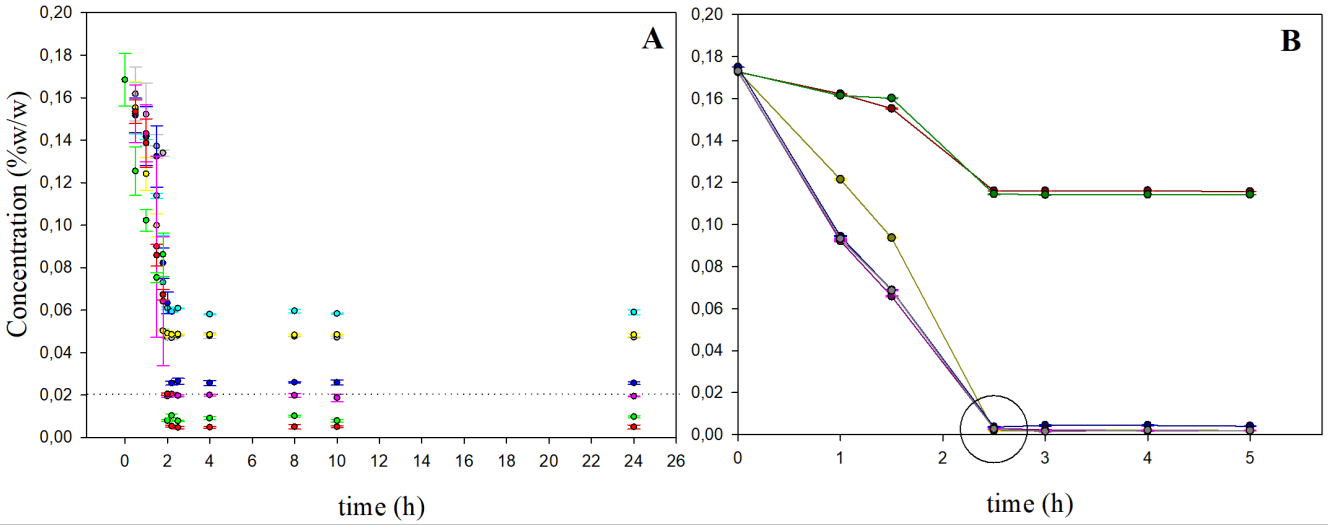

Figure 4: Adsorption profiles for free glycerin on (A): AC-600-90 (●), AC-800-90 (●), AC-800-30 (●), AC-H_3PO_4-50% (●), AC-H_3PO_4-85% (●), AC-KOH-1:3 (●), and AC-KOH-1:1 (●); and determination of the optimum mass of AC-KOH-1:1 (B) for concentrations of 0.1% (●), 0.25% (●), 0.5% (●), 1.0% (●), 2.0% (●), and 3.0% (●). The dashed line indicates the permissible limit of free glycerol according to ISO 14214-1.

a p-value of 0.0001 for a significance level of 0.05, indicating a high statistical significance in the relationship between the experimental data and the model. This means that the probability of the obtained fit being due to chance is low (0.01%), suggesting that the Freundlich model adequately describes the adsorption under the evaluated conditions. However, a low p-value does not necessarily imply that Freundlich is the best model, but rather that the correlation between the data and the Freundlich equation is statistically significant.

3.5.3 Langmuir–Freundlich Isotherm

This isotherm considers certain characteristics of both the Langmuir and Freundlich isotherms, where the maximum adsorption capacity can be determined by considering the existence of different types of adsorption sites on the surface of the solid [59]. Equation 5 expresses its behavior:

$$q_e = \frac{q_m(K_{LF}C_e)^{n_{LF}}}{1 + (K_{LF}C_e)^{n_{LF}}} \tag{5}$$

The isotherm is a three-parameter model, where K_{LF} is the affinity constant (L/mg), n_{LF} is known as the heterogeneity index and the q_m is the maximum amount per adsorbent (mg/g). In Table 2, a p-value of < 0.0001 is presented for a significance level of 0.05, and a correlation coefficient value of 0.76 ± 0.02, showing that there is a statistically significant correlation between the data and the combined equation.

3.5.4 Redlich–Peterson (R–P) isotherm

This equation considers characteristics of both Langmuir and Freundlich, and it is expressed according to Equation 6:

$$q_e = \frac{q_m(K_{RP}C_e)}{1 + (K_{RP}C_e)^{n_{RP}}} \tag{6}$$

To obtain the value of n_{RP}, an adimensional equation expressed according to Equation 7 should be used [60]:

$$\frac{q_e}{q_{ref}} = \left(\frac{C_e}{C_{ref}}\right) \frac{\left(\frac{1}{K_{RP}C_{ref}^{n_{RP}}} + 1\right)}{\left(\frac{1}{K_{RP}C_{ref}^{n_{RP}}}\right)\left(\frac{C_e}{C_{ref}}\right)^{n_{RP}}} \tag{7}$$

Where C_{ref} is the value of the highest concentration at equilibrium, and the value of q_{ref} is the highest value of the maximum amount that the adsorbent should adsorb at equilibrium, K_{RP} is the constant in the R–P isotherm, and n_{RP} is an exponent like the Freundlich model (The range of values for n_{RP} is within the interval $0 < n_{RP} < 1$). Afterward, the equation is rearranged into a linear form, applying Equation 8:

$$\frac{C_e}{q_e} = \frac{1}{K_{RP}q_m} + \frac{1}{q_m}C_e^{n_{RP}} \tag{8}$$

A regression analysis yields the values of q_m y K_{RP}.

From the nonlinear regression for the R–P isotherm, the obtained values for the parameter n_{RP} were 1.32 ± 0.01 for free glycerol (see Table 2), and the correlation coefficient is 0.79. The no linear R–P equation for the experimental data presented a coefficient correlation value of 0.78 ± 0.00.

Therefore, to determine which model best describes the adsorption process, it is essential to compare other goodness-of-fit parameters such as the correlation coefficient, the adjusted coefficient, and the standard error of the estimate. According to the results presented in Table 2 for the isotherm model fitting analysis (Langmuir, Freundlich, Langmuir–Freundlich, and Redlich–Peterson), it was determined that the Langmuir–Freundlich and Langmuir models exhibited a similar fit, with R^2 values of 0.76 and Adj Sqr close to 0.73, indicating a good fit, although with an SEE of approximately 1.03, suggesting some data dispersion. On the other hand, the Freundlich model showed the lowest fit (R^2 = 0.61, Adj Sqr = 0.586, and SEE = 1.28) indicating that the adsorption does not follow completely heterogeneous behavior. In contrast, the Redlich–Peterson model exhibited the best performance, with R^2 and Adj Sqr values very close (0.78 and 0.783), along with the lowest SEE (0.927), suggesting that this model more accurately describes the adsorption equilibrium, reaching a maximum adsorption capacity of approximately 11.35 mg of glycerin per gram of activated carbon.

However, it is important to emphasize that the nonlinear fitting (Equation 6) of the isotherm must consider the n_{RP} constant, which is obtained from the dimensionless equation (Equation 7). The superiority of this model can be attributed to its hybrid nature, combining features of both Langmuir and Freundlich models, allowing greater

Table 2: Calculated parameters from the experimental results obtained for the Langmuir, Freundlich, Langmuir-Freundlich and Redlich-Peterson.

Isotherm	Parameter	Values	P-value	Adj R^2	SEE
Langmuir	q_m (mg/g)	5.78 ± 0.03	< 0.0001	0.733	1.03
	K_L (L/mg)	1.78 ± 0.08			
	R^2	0.76 ± 0.01			
Freundlich	K_F (mg/g)	2.88 ± 0.02	0.0001	0.586	1.28
	n	3.48 ± 0.06			
	R^2	0.61 ± 0.00			
Langmuir–Freundlich	q_m (mg/g)	5.43 ± 0.06	< 0.0001	0.730	1.03
	K_{LF} (L/mg)	2.20 ± 0.09			
	n_{LF}	1.36 ± 0.13			
	R^2	0.76 ± 0.02			
Redlich–Peterson (non-linear, n_{RP} = 1.32)	q_m (mg/g)	11.35 ± 0.01	< 0.0001	0.783	0.927
	K_{RP} (L/mg)	0.59 ± 0.01			
	R^2	0.78 ± 0.00			
Redlich–Peterson (dimensionless)	n_{RP}	1.32 ± 0.01	< 0.0001	0.783	0.186
	R^2 for n_{RP}	0.79 ± 0.03			
Redlich–Peterson (linear)	q_m (L/mg)	11.63 ± 0.00	< 0.0001	0.982	0.093
	K_{RP} (mg/g)	0.44 ± 0.00			
	R^2	0.98 ± 0.00			

*SEE: Standard Error of the Estimate; Adj Rsqr: Adjusted R-Squared

flexibility to describe both homogeneous and heterogeneous surfaces. Additionally, the low SEE indicates that the model's predictions have less error compared to the experimental values, supporting its suitability for describing glycerin adsorption onto the studied activated carbon. In this regard, the selection of the most appropriate model should not be based solely on the R^2 value but also on the model's ability to represent the interaction between the adsorbate and adsorbent under specific experimental conditions. The good fit of the glycerin adsorption data to the Redlich-Peterson model suggests that the process combines characteristics of both Langmuir and Freundlich models, indicating that adsorption involves both homogeneous and heterogeneous sites. Thus, the process may exhibit saturation in adsorption, as described by Langmuir, while also displaying variability in adsorption sites, like Freundlich, enabling a better understanding of the interaction between glycerin and the adsorbent material. Several studies have investigated glycerin adsorption on activated carbon, but none specifically report fitting to the Redlich-Peterson isotherm. Most of the research in this field has used models such as Langmuir and Freundlich to describe the adsorption equilibrium. In studies reported using raw sugarcane, the experimental data fitted the Langmuir isotherm, reporting values of 88.96 mg/g for q_m. Comparing them with the results obtained in the present study, raw sugarcane bagasse exhibited a higher capacity for adsorption of free glycerol in the biodiesel sample [2]. Similarly, the use of resins for the adsorption of free glycerol has been reported; one of them is the resin modified by sulfonation of Amberlite XAD1180 at adsorption temperatures of 30 °C. The experimental data fitted the Langmuir isotherm with an R^2 of 0.98 and q_m of 434.8 mg/g, which are higher than the parameters found in the present study, but with the disadvantage of increased cost in resin modification [61]. In this field of research, there are very few equilibrium and kinetics studies proposed for the analysis of contaminants in biodiesel using dry washing.

3.6 Adsorption kinetics

The study of the kinetic behavior of the free glycerol adsorption process on AC-KOH-1:1 was analyzed using the pseudo-first-order and pseudo-second-order equations; for this, the adsorption capacity over time (qt) and adsorption time (t) were considered.

3.6.1 Pseudo first-order model

Equation 9 describes the pseudo-first-order model, which indicates the adsorption behavior of the adsorbent by the adsorbate at the time.

$$q_t = q_e\left(1 - e^{-k_1 t}\right) \tag{9}$$

Where k_1 is the first-order kinetic constant (1/h) and q_e is the amount of solute per mass of adsorbent at equilibrium (mg/g).

A nonlinear regression was applied to calculate q_e y k_1 for different ratios of activated carbon used in the removal of free glycerol in the biodiesel sample. The pseudo-first-order kinetic behavior is shown in Table 3.

The correlation coefficients for the pseudo-first-order model in the experimental data are 0.86 ± 0.002 when 0.1 % of activated carbon is used and 0.97 ± 0.003 for the carbon concentration at 3.0 %, with a p-value below 0.05; therefore, the pseudo-first-order equation provided a good fit to the experimental data. Additionally, the value of the equilibrium adsorption capacity (q_e) predicted by the pseudo-first-order equation was close to the experimental values as observed in Table 3.

3.7 Pseudo second order model

Experimental results were analyzed using Equation 10:

$$\frac{t}{q_t} = \frac{1}{k_2 q_e^2} + \frac{1}{q_e}\, t \tag{10}$$

The solute amount per mass of adsorbent at equilibrium (q_e) is expressed in (mg/g), and the value of k_2 is expressed in (g/mg·h), being the rate constant of pseudo-second-order chemical sorption equilibrium. For the experimental data, the correlation coefficient of the fit ranged from 0.17 ± 0.02 to 0.92 ± 0.00 for the lowest and highest mass of activated carbon AC-KOH-1:1, indicating that this fit is not the most appropriate when concentrations below 0.5 % of activated carbon are used. The estimated q_e value at concentrations below 1 % differs considerably from the experimental q_e value, indicating that it does not fit the pseudo-second-order model.

Table 3: Kinetic parameters for the adsorption of free glycerol using activated carbon

Ca (%)[a]	C_0 (mg/L)[b]	q_e exp	Pseudo-first-order kinetics				Pseudo-second-order kinetics			
			q_e (mg/g)	k_1 (h^{-1})	R^2	p-value	q_e (mg/g)	k_2 (h^{-1})	R^2	p-value
0.1	15.14	4.99 ± 0.01	7.28 ± 0.05	0.289 ± 0.004	0.86 ± 0.002	0.003	10.45 ± 0.43	0.019 ± 0.002	0.17 ± 0.02	0.292
0.25	15.16	5.35 ± 0.01	7.60 ± 0.05	0.296 ± 0.003	0.93 ± 0.002	0.0005	8.97 ± 0.08	0.035 ± 0.001	0.39 ± 0.01	0.137
0.5	15.20	3.00 ± 0.01	3.72 ± 0.01	0.428 ± 0.003	0.92 ± 0.004	0.0006	4.11 ± 0.02	0.145 ± 0.004	0.68 ± 0.01	0.023
1.0	15.34	1.50 ± 0.00	1.65 ± 0.00	0.646 ± 0.006	0.97 ± 0.005	< 0.0001	1.73 ± 0.00	0.810 ± 0.010	0.92 ± 0.00	0.006
2.0	15.16	0.75 ± 0.00	0.82 ± 0.00	0.647 ± 0.002	0.97 ± 0.003	< 0.0001	0.86 ± 0.00	1.630 ± 0.010	0.92 ± 0.00	0.001
3.0	15.18	0.50 ± 0.00	0.55 ± 0.00	0.632 ± 0.003	0.97 ± 0.003	< 0.0001	0.58 ± 0.00	2.320 ± 0.030	0.92 ± 0.00	0.001

[a] C_a: Concentration of AC-KOH-1:1
[b] C_0: Initial concentration of free glycerol

Thus, it is concluded that the kinetic behavior of activated carbon with KOH in a 1:1 molar ratio for the adsorption of free glycerol in a biodiesel sample exhibits pseudo-first-order behavior, indicating a solid/liquid system depending on the available sites on the surface of the activated carbon for a physisorption process. No reports were found in the literature of kinetic studies for the adsorption of contaminants in a biodiesel sample using activated carbon; however, an adjustment to the pseudo-second-order kinetics was reported using raw sugarcane bagasse, although the correlation coefficient was 0.89, which is far from unity, and the p-value values were not reported.

3.8 Biodiesel purification

The free glycerol content in the biodiesel before purification was 0.16 ± 0.05 % w/w. This value was higher than that reported by other authors under similar production conditions from WFO (0.01 ± 0.00 % w/w) and soybean oil (0.03 ± 0.00 % w/w) [2]. Table 4 shows the physicochemical parameters for biodiesel purification by conventional and dry washing. It was determined that for dry washing, all parameters established by ISO 14214-1 were met, while for conventional washing, the viscosity value exceeded the standards (3.5-5.0 mm^2/s), with a value of 5.70 ±0.05 mm^2/s; additionally, a yield percentage of 98 % was determined; however, the data obtained by both methods showed significant differences, with a p-value below 0.05, concluding that the biodiesel purification process with dry washing, using AC-KOH-1:1 from coffee husks, results in an interesting alternative for the removal of free glycerol from biodiesel. Other studies reported free glycerol concentration of 0.01 ± 0.00 % w/w, density of 880 ± 16 kg/m3, acidity index of 0.29 ± 0.03 mgKOH/g and viscosity of 4.5 ± 0.1 mm^2/s using adsorbent material from sugarcane[2]. Higher values than those in the present study were also reported when using activated carbon from oil palm seeds, with an acidity index of 0.19 ± 0.02 mgKOH/g and free glycerol concentration of 0.020 ± 0.008 % w/w [62]. Meanwhile, in studies conducted with activated carbon from rice husks, results like those determined in this research were obtained, with free glycerol values of 0.004 ± 0.001 % w/w and an acidity index of 0.13 ± 0.02 mgKOH/g [56].

Table 4: Comparison of biodiesel quality parameters after conventional and dry washing

Parameter	Conventional washing	Dry washing	ISO 14214-1	p-value
Acidity index (mgKOH/g)	0.193 ± 0.001	0.119 ± 0.001	0.5 max	< 0.001
Density (kg/m^3)	870.4 ± 0.2	868.5 ± 0.1	860–900	0.013
Humidity and volatile matter (mg/kg)	10.46 ± 0.09	12.4 ± 0.1	24 max	< 0.001
Viscosity (mm^2/s)	5.70 ± 0.05	4.4 ± 0.1	3.5–5.0	0.002
Free glycerol (% w/w)	0.015 ± 0.002	0.002 ± 0.000	0.02 max	0.002
Efficiency (%)	98.0			

4 Conclusions

According to the analysis of the activation process, it was determined that the optimal treatment for the coffee husk was chemical activation with KOH at a ratio of 1:1 carbon: KOH (AC-KOH-1:1). The optimal mass of the adsorbent showed a ratio of 0.05 % and a contact time of 2.5 h, achieving removal of free glycerol greater than 98 % and complying with the standards established in ISO 14214-1. The characterization of the carbon showed that AC-KOH-1:1 differed from the other activated carbons obtained in the present work. UV-Vis and NIR analyses revealed a pronounced peak around 260 nm, associated with oxygenated compounds such as water and nitrogenates. Likewise, characterization by cyclic voltammetry indicated an increase in the electroactive area, suggesting higher electrical conductivity. An activated carbon with high electrical conductivity typically contains a greater number of oxygenated functional groups, such as carbonyls, hydroxyls, and carboxyls, which can interact with glycerin through hydrogen bonding or electrostatic attraction. These groups increase the polarity of the carbon surface, enhancing the adsorption of polar molecules like glycerin.

On the other hand. The BET analysis presented a combination of type I and IV isotherms, indicating Langmuir's behavior with hysteresis, expressing a micropore and mesopore pore size distribution. Therefore, these analyses are related to equilibrium behavior and adsorption kinetics, in which the experimental equilibrium data were described by the Langmuir isotherm, with a correlation coefficient value of 0.87 ± 0.01 and a p-value of 0.02. The maximum adsorption capacity of free glycerol was determined to be 5.78 ± 0.03 mg/g, indicating a homogeneous surface and a uniform distribution of adsorption heat. Similarly, in the kinetic study, it was defined that the obtained data fitted the pseudo-first-order model, indicating that the rate-limiting step could be physisorption. Finally, comparing the biodiesel purification processes, it was determined that the highest removal of free glycerol was achieved through dry washing, with a final solution value of 0.002 ± 0.000% w/w, while in conventional washing it was 0.015 ± 0.002% w/w. Thus, it can be concluded that the dry washing method, using coffee husks, is an interesting alternative as it adds value to agro-industrial waste as potential adsorbents. Additionally, this process reduces water consumption and therefore the volumes of wastewater that need to be treated.

Acknowledgments

The authors wish to thank the public universities, especially for the support of the Universidad de la Amazonia and for the financial support provided by the Vice-Rectorate for Research of the Uni-versidad del Cauca through the call "Call for support for research theses within the framework of Master's, Doctorate, and Medical-Surgical Specialty Programs," funding the project with ID 5951. They also wish to thank the National University of La Plata in Ar-gentina and the government for making academic training possible and advancing scientific knowledge in vulnerable regions.

Author contributions

All authors contributed equally to the development and final writing of this paper. Nasly Delgado, Jaime Martínez, and Enna Mejía

participated jointly in the initial conception of the study, the design of the methodology, the development of the research, the acquisition and analysis of results, and the drafting and critical revision of the manuscript. All authors reviewed and approved the final version of the paper.

Conflict of interest

The authors declare that there is no conflict of interest. This manuscript was developed, prepared, and reviewed collaboratively by all authors, who contributed substantially to its conception, analysis, and final approval. No financial, personal, or professional relationships influenced the content of this work.

References

[1] A. Z. Rueda and M. Y. Ahumada, Biodiésel de palma colombiano: de la ficción energética a la realidad de un negocio. Bogotá, Colombia: Fedepalma, 2013.

[2] M. J. Alves, Í. V. Cavalcanti, M. M. de Resende, V. L. Cardoso, and M. H. Reis, "Biodiesel dry purification with sugarcane bagasse," Industrial Crops and Products, vol. 89, pp. 119–127, 2016, doi: 10.1016/j.indcrop.2016.05.005.

[3] S. Gopalakrishnan, J. Ubaidullah, P. Shanmugasundaram, K. Yuvaraj, and T. Tamilarasu, "Production of biodiesel from used cooking oil," International Journal for Innovative Research in Science and Technology, pp. 90–95, Apr. 2017.

[4] N. Banerjee, R. Ramakrishnan, and T. Jash, "Biodiesel production from used vegetable oil collected from shops selling fritters in Kolkata," Energy Procedia, vol. 54, pp. 161–165, 2014, doi: 10.1016/j.egypro.2014.07.259.

[5] A. Bouaid, R. Vázquez, M. Martinez, and J. Aracil, "Effect of free fatty acids contents on biodiesel quality: Pilot plant studies," Fuel, vol. 174, pp. 54–62, 2016, doi: 10.1016/j.fuel.2016.01.018.

[6] B. Murcia Ordoñez, L. C. Chaves, M. A. Murcia, W. Rodríguez Pérez, and E. R. Alvarado, "Caracterización de biodiesel obtenido de aceite residual de cocina," Revista Colombiana de Biotecnología, vol. XV, no. 1, pp. 61–70, 2013.

[7] D. Singh, D. Sharma, S. L. Soni, C. S. Inda, S. Sharma, P. K. Sharma, and A. Jhalani, "A comprehensive review of biodiesel production from waste cooking oil and its use as fuel in compression ignition engines: 3rd generation cleaner feedstock," Journal of Cleaner Production, vol. 307, Art. no. 127299, 2021, doi: 10.1016/j.jclepro.2021.127299.

[8] D. Singh, D. Sharma, S. L. Soni, S. Sharma, P. K. Sharma, and A. Jhalani, "A review of feedstocks, production processes, and yield for different generations of biodiesel," Fuel, vol. 262, Art. no. 116553, 2020, doi: 10.1016/j.fuel.2019.116553.

[9] M. Mofijur, S. Y. A. Siddiki, M. B. A. Shuvho, F. Djavanroodi, I. M. R. Fattah, H. C. Ong, M. A. Chowdhury, and T. M. I. Mahlia, "Effect of nanocatalysts on the transesterification reaction of first, second and third generation biodiesel sources: A mini-review," Chemosphere, vol. 270, Art. no. 128642, 2021, doi: 10.1016/j.chemosphere.2020.128642.

[10] R. V. Quah, Y. H. Tan, N. M. Mubarak, M. Khalid, E. C. Abdullah, and C. Nolasco-Hipolito, "An overview of biodiesel production using recyclable biomass and non-biomass derived magnetic catalysts," Journal of Environmental Chemical Engineering, vol. 7, no. 4, Art. no. 103219, 2019, doi: 10.1016/j.jece.2019.103219.

[11] M. G. Gomes, D. Q. Santos, L. C. de Morais, and D. Pasquini, "Purification of biodiesel by dry washing, employing starch and cellulose as natural adsorbents," Fuel, vol. 155, pp. 1–6, 2015, doi: 10.1016/j.fuel.2015.04.012.

[12] N. Tshizanga, E. F. Aransiola, and O. Oyekola, "Optimisation of biodiesel production from waste vegetable oil and eggshell ash," South African Journal of Chemical Engineering, vol. 23, pp. 145–156, 2017, doi: 10.1016/j.sajce.2017.05.003.

[13] C. S. Faccini, M. E. da Cunha, M. S. A. Moraes, L. C. Krause, M. C. Manique, M. R. A. Rodrigues, E. V. Benvenutti, and E. B. Caramão, "Dry washing in biodiesel purification: A comparative study of adsorbents," Journal of the Brazilian Chemical Society, vol. 22, no. 3, pp. 558–563, 2011, doi: 10.1590/S0103-50532011000300021.

[14] B. Hamed, A. Saraeian, C. Able, and K. Karimi, "Biodiesel purification and upgrading technologies," in Green Energy and Technology. Cham, Switzerland: Springer, 2019, ch. 18, doi: 10.1007/978-3-030-11599-9_18.

[15] S. Nitiéma-Yefanova, R. Richard, S. Thiebaud-Roux, B. Bouyssiere, Y. L. Bonzi-Coulibaly, R. H. C. Nébié, K. Mozet, and L. Coniglio, "Dry purification by natural adsorbents of ethyl biodiesels derived from nonedible oils," Energy & Fuels, vol. 29, no. 1, pp. 150–159, 2015, doi: 10.1021/ef501365u.

[16] N. Delgado, D. Marino, A. Capparelli, J. C. Casas-Zapata, and A. Navarro, "Pharmaceutical compound removal using down-flow fixed bed filters with powder activated carbon: A novel configuration," Journal of Environmental Chemical Engineering, vol. 10, no. 3, Art. no. 107706, 2022, doi: 10.1016/j.jece.2022.107706.

[17] Y. A. B. Neolaka, A. A. P. Riwu, U. O. Aigbe, K. E. Ukhurebor, R. B. Onyancha, H. Darmokoesoemo, and H. S. Kusuma, "Potential of activated carbon from various sources as a low-cost adsorbent to remove heavy metals and synthetic dyes," Results in Chemistry, vol. 5, Art. no. 100711, 2023, doi: 10.1016/j.rechem.2022.100711.

[18] M. Sultana, M. H. Rownok, M. Sabrin, M. H. Rahaman, and S. M. N. Alam, "A review on experimental chemically modified activated carbon to enhance dye and heavy metals adsorption," Cleaner Engineering and Technology, vol. 6, Art. no. 100382, 2022, doi: 10.1016/j.clet.2021.100382.

[19] D. T. Bekele, N. T. Shibeshi, and A. S. Reshad, "Fatty acid methyl esters production from crude waste frying oil using modified coffee husk ash catalyst: Parameters optimization," Results in Engineering, vol. 20, Art. no. 101627, 2023, doi: 10.1016/j.rineng.2023.101627.

[20] S. A. E. A. Ismail and R. F. M. Ali, "Physico-chemical properties of biodiesel manufactured from waste frying oil using domestic adsorbents," Science and Technology of Advanced Materials, vol. 16, no. 3, Art. no. 034602, 2015, doi: 10.1088/1468-6996/16/3/034602.

[21] N. K. Keppy, G. Bain, and M. W. Allen, "Determination of free glycerol in biodiesel with the Evolution Array UV–Visible spectrophotometer," Thermo Fisher Scientific, Application Note AN-51853, 2009. [Online]. Available: https://tools.thermofisher.com

[22] P. Bondioli and L. Della Bella, "An alternative spectrophotometric method for the determination of free glycerol in biodiesel," European Journal of Lipid Science and Technology, vol. 107, no. 3, pp. 153–157, 2005, doi: 10.1002/ejlt.200401054.

[23] V. Boonamnuayvitaya, S. Sae-Ung, and W. Tanthapanichakoon, "Preparation of activated carbons from coffee residue for the adsorption of formaldehyde," Separation and Purification Technology, vol. 42, no. 2, pp. 159–168, 2005, doi: 10.1016/j.seppur.2004.07.007.

[24] L. C. A. Oliveira, E. Pereira, I. R. Guimarães, A. Vallone, M. Pereira, J. P. Mesquita, and K. Sapag, "Preparation of activated carbons from coffee husks utilizing $FeCl_3$ and $ZnCl_2$ as activating agents," Journal of Hazardous Materials, vol. 165, nos. 1–3, pp. 87–94, 2009, doi: 10.1016/j.jhazmat.2008.09.064.

[25] Q. Yu, M. Li, H. Zhao, and C. Wu, "Preparation of coffee-shell activated carbon and its application for water vapor adsorption," Renewable Energy, vol. 142, pp. 11–19, 2019, doi: 10.1016/j.renene.2019.04.097.

[26] N. F. Tehrani, J. S. Aznar, and Y. Kiros, "Coffee extract residue for production of ethanol and activated carbons," Journal of Cleaner Production, vol. 91, pp. 64–70, 2015, doi: 10.1016/j.jclepro.2014.12.031.

[27] E. R. Mejía Silva, Caracterización del aceite usado y el biodiésel producido en el Tecnoparque Agroecológico Yamboró (SENA-Pitalito), Trabajo de grado, Universidad de la Amazonia, Florencia, Colombia, 2014.

[28] M. Harabi, S. Neji Bouguerra, F. Marrakchi, L. P. Chrysikou, S. Bezergianni, and M. Bouaziz, "Biodiesel and crude glycerol from waste frying oil: Production, characterization and evaluation of biodiesel oxidative stability with diesel blends," Sustainability, vol. 11, no. 7, Art. no. 1937, 2019, doi: 10.3390/su11071937.

[29] F. Binhweel, M. Bahadi, H. Pyar, A. Alsaedi, S. Hossain, and M. I. Ahmad, "A comparative review of some physicochemical properties of biodiesels synthesized from different generations of vegetative oils," Journal of Physics: Conference Series, vol. 1900, no. 1, Art. no. 012009, 2021, doi: 10.1088/1742-6596/1900/1/012009.

[30] C. Medeiros Vicentini-Polette, P. Rodolfo Ramos, C. Bernardo Gonçalves, and A. Lopes de Oliveira, "Determination of free fatty acids in crude vegetable oil samples obtained by high-pressure processes," Food Chemistry: X, vol. 12, Art. no. 100166, 2021, doi: 10.1016/j.fochx.2021.100166.

[31] Z. Al-Hamamre and J. Yamin, "Parametric study of the alkali catalyzed transesterification of waste frying oil for biodiesel production," Energy Conversion and Management, vol. 79, pp. 246–254, 2014, doi: 10.1016/j.enconman.2013.12.027.

[32] M. A. H. Shaah, M. S. Hossain, F. A. S. Allafi, A. Alsaedi, N. Ismail, M. O. Ab Kadir, and M. I. Ahmad, "A review on non-edible oil as a potential feedstock for biodiesel: Physicochemical properties and production technologies," RSC Advances, vol. 11, no. 40, pp. 25018–25037, 2021, doi: 10.1039/d1ra04311k.

[33] G. Debaene, A. Ukalska-Jaruga, B. Smreczak, and E. Papierowska, "Diffuse reflectance spectroscopy for black carbon screening of agricultural soils under industrial anthropopressure," Molecules, vol. 27, no. 21, Art. no. 7334, 2022, doi: 10.3390/molecules27217334.

[34] K. B. Beć and C. W. Huck, "Breakthrough potential in near-infrared spectroscopy: Spectra simulation. A review of recent developments," Frontiers in Chemistry, vol. 7, Art. no. 48, 2019, doi: 10.3389/fchem.2019.00048.

[35] S.-W. Hwang, U. T. Hwang, K. Jo, T. Lee, J. Park, J.-C. Kim, H. W. Kwak, I.-G. Choi, and H. Yeo, "NIR-chemometric approaches for evaluating carbonization characteristics of hydrothermally carbonized lignin," Scientific Reports, vol. 11, no. 1, Art. no. 16979, 2021, doi: 10.1038/s41598-021-96461-x.

[36] M. Mäkelä and P. Geladi, "Hyperspectral near infrared imaging quantifies the heterogeneity of carbon materials," Scientific Reports, vol. 8, no. 1, Art. no. 10442, 2018, doi: 10.1038/s41598-018-28889-7.

[37] D. Li and L. Li, "Detection of water pH using visible near-infrared spectroscopy and one-dimensional convolutional neural network," Sensors, vol. 22, no. 15, Art. no. 5809, 2022, doi: 10.3390/s22155809.

[38] X. Qi, Y. Lian, L. Xie, Y. Wang, and Z. Lu, "Water quality detection based on UV–Vis and NIR spectroscopy: A review," Applied Spectroscopy Reviews, pp. 1–25, 2023, doi: 10.1080/05704928.2023.2294458.

[39] J. Njuguna, O. A. Vanli, and R. Liang, "A review of spectral methods for dispersion characterization of carbon nanotubes in aqueous suspensions," Journal of Spectroscopy, vol. 2015, Art. no. 463156, 2015, doi: 10.1155/2015/463156.

[40] K. Sathish-Kumar, G. Vázquez-Huerta, A. Rodríguez-Castellanos, H. M. Poggi-Varaldo, and O. Solorza-Feria, "Microwave assisted synthesis and characterizations of decorated activated carbon," International Journal of Electrochemical Science, vol. 7, no. 6, pp. 5484–5494, 2012.

[41] S. Castan, G. Sigmund, T. Hüffer, N. Tepe, F. von der Kammer, B. Chefetz, and T. Hofmann, "The importance of aromaticity to describe the interactions of organic matter with carbonaceous materials depends on molecular weight and sorbent geometry," Environmental Science: Processes & Impacts, vol. 22, no. 9, pp. 1888–1897, 2020, doi: 10.1039/D0EM00267D.

[42] C.-H. Liu, W. Chu, H. Li, S. A. Boyd, B. J. Teppen, J. Mao, J. Lehmann, and W. Zhang, "Quantification and characterization of dissolved organic carbon from biochars," Geoderma, vol. 335, pp. 161–169, 2019, doi: 10.1016/j.geoderma.2018.08.019.

[43] R. Zeng, C. M. Mannaerts, and C. Lievens, "Assessment of UV–Vis spectra analysis methods for quantifying the absorption properties of chromophoric dissolved organic matter (CDOM)," Frontiers in Environmental Science, vol. 11, Art. no. 1152536, 2023, doi: 10.3389/fenvs.2023.1152536.

[44] N. Elgrishi, K. J. Rountree, B. D. McCarthy, E. S. Rountree, T. T. Eisenhart, and J. L. Dempsey, "A practical beginner's guide to cyclic voltammetry," Journal of Chemical Education, vol. 95, no. 2, pp. 197–206, 2018, doi: 10.1021/acs.jchemed.7b00361.

[45] E. Pollak, N. Levy, L. Eliad, G. Salitra, A. Soffer, and D. Aurbach, "Review on engineering and characterization of activated carbon electrodes for electrochemical double layer capacitors and separation processes," Israel Journal of Chemistry, vol. 48, nos. 3–4, pp. 287–303, 2008, doi: 10.1560/IJC.48.3-4.287.

[46] F.-C. Wu, R.-L. Tseng, C.-C. Hu, and C.-C. Wang, "Physical and electrochemical characterization of activated carbons prepared from fir woods for supercapacitors," Journal of Power Sources, vol. 138, no. 1, pp. 351–359, 2004, doi: 10.1016/j.jpowsour.2004.06.023.

[47] M. Sivachidambaram, J. J. Vijaya, L. J. Kennedy, R. Jothiramalingam, H. A. Al-Lohedan, M. A. Munusamy, E. Elanthamilan, and J. P. Merlin, "Preparation and characterization of activated carbon derived from Borassus flabellifer flower as an electrode material for supercapacitor applications," New Journal of Chemistry, vol. 41, no. 10, pp. 3939–3949, 2017, doi: 10.1039/C6NJ03867K.

[48] N. Festinger, K. Morawska, V. Ivanovski, M. Ziąbka, K. Jedlińska, W. Ciesielski, and S. Smarzewska, "Comparative electroanalytical studies of graphite flake and multilayer graphene paste electrodes," Sensors, vol. 20, no. 6, Art. no. 1684, 2020, doi: 10.3390/s20061684.

[49] J. C. Forero, E. Roa, J. G. Reyes, C. Acevedo, and N. Osses, "Development of useful biomaterial for bone tissue engineering by incorporating nano-copper–zinc alloy (nCuZn) in chitosan/gelatin/nano-hydroxyapatite scaffold," Materials, vol. 10, no. 10, Art. no. 1177, 2017, doi: 10.3390/ma10101177.

[50] A. A. Awe, B. O. Opeolu, O. S. Fatoki, O. S. Ayanda, V. A. Jackson, and R. Snyman, "Preparation and characterisation of activated carbon from Vitis vinifera leaf litter and its adsorption performance for aqueous phenanthrene," Applied Biological Chemistry, vol. 63, no. 1, Art. no. 12, 2020, doi: 10.1186/s13765-020-00494-1.

[51] A. Forouzanfar, P. Hasanpour, Y. Yazdandoust, H. Bagheri, and H. S. Mohammadipour, "Evaluating the effect of active charcoal-containing toothpaste on color change, microhardness, and surface roughness of tooth enamel and resin composite restorative materials," International Journal of Dentistry, vol. 2023, Art. no. 6736623, 2023, doi: 10.1155/2023/6736623.

[52] Z. Yang, X. Ju, H. Liao, Z. Meng, H. Ning, Y. Li, Z. Chen, and J. Long, "Preparation of activated carbon doped with graphene oxide porous materials and their high gas adsorption performance," ACS Omega, vol. 6, no. 30, pp. 19799–19810, 2021, doi: 10.1021/acsomega.1c02416.

[53] E. E. Abdel-Hady, H. F. M. Mohamed, S. H. M. Hafez, A. M. M. Fahmy, A. Magdy, A. S. Mohamed, E. O. Ali, H. R. Abdelhamed, and O. M. Mahmoud, "Textural properties and

adsorption behavior of Zn–Mg–Al layered double hydroxide upon crystal violet dye removal as a low-cost, effective, and recyclable adsorbent," Scientific Reports, vol. 13, no. 1, Art. no. 6435, 2023, doi: 10.1038/s41598-023-33142-x.

[54] M. G. Gomes, D. Q. Santos, L. C. de Morais, and D. Pasquini, "Purification of biodiesel by dry washing and the use of starch and cellulose as natural adsorbents: Part II—Study of purification times," Biofuels, pp. 1–9, 2018, doi: 10.1080/17597269.2018.1510721.

[55] L. C. dos Santos, O. F. H. Adarme, B. E. L. Baêta, L. V. A. Gurgel, and S. F. de Aquino, "Production of biogas (methane and hydrogen) from anaerobic digestion of hemicellulosic hydrolysate generated in the oxidative pretreatment of coffee husks," Bioresource Technology, vol. 263, pp. 601–612, 2018, doi: 10.1016/j.biortech.2018.05.037.

[56] M. C. Manique, C. S. Faccini, B. Onorevoli, E. V. Benvenutti, and E. B. Caramão, "Rice husk ash as an adsorbent for purifying biodiesel from waste frying oil," Fuel, vol. 92, no. 1, pp. 56–61, 2012, doi: 10.1016/j.fuel.2011.07.024.

[57] S. Sun, Q. Yu, M. Li, H. Zhao, and C. Wu, "Preparation of coffee-shell activated carbon and its application for water vapor adsorption," Renewable Energy, vol. 142, pp. 11–19, 2019, doi: 10.1016/j.renene.2019.04.097.

[58] E. N. El Qada, S. J. Allen, and G. M. Walker, "Adsorption of methylene blue onto activated carbon produced from steam-activated bituminous coal: A study of equilibrium adsorption isotherm," Chemical Engineering Journal, vol. 124, nos. 1–3, pp. 103–110, 2006, doi: 10.1016/j.cej.2006.08.015.

[59] N. Delgado, A. Capparelli, A. Navarro, and D. Marino, "Pharmaceutical emerging pollutants removal from water using powdered activated carbon: Study of kinetics and adsorption equilibrium," Journal of Environmental Management, vol. 236, pp. 301–308, 2019, doi: 10.1016/j.jenvman.2019.01.116.

[60] F.-C. Wu, B.-L. Liu, K.-T. Wu, and R.-L. Tseng, "A new linear form analysis of Redlich–Peterson isotherm equation for the adsorptions of dyes," Chemical Engineering Journal, vol. 162, no. 1, pp. 21–27, 2010, doi: 10.1016/j.cej.2010.03.006.

[61] B. Chen, W. Wang, X. Liu, W. Xue, X. Ma, G. Chen, Q. Yu, and R. Li, "Adsorption study of glycerol in biodiesel on the sulfonated adsorbent," Industrial & Engineering Chemistry Research, vol. 51, no. 39, pp. 12933–12939, 2012, doi: 10.1021/ie301951p.

[62] M. A. Ahmad Farid, M. A. Hassan, Y. H. Taufiq-Yap, Y. Shirai, M. Y. Hasan, and M. R. Zakaria, "Waterless purification using oil palm biomass-derived bioadsorbent improved the quality of biodiesel from waste cooking oil," Journal of Cleaner Production, vol. 165, pp. 262–272, 2017, doi: 10.1016/j.jclepro.2017.07.136.

Supplementary Material
Supplementary Figures

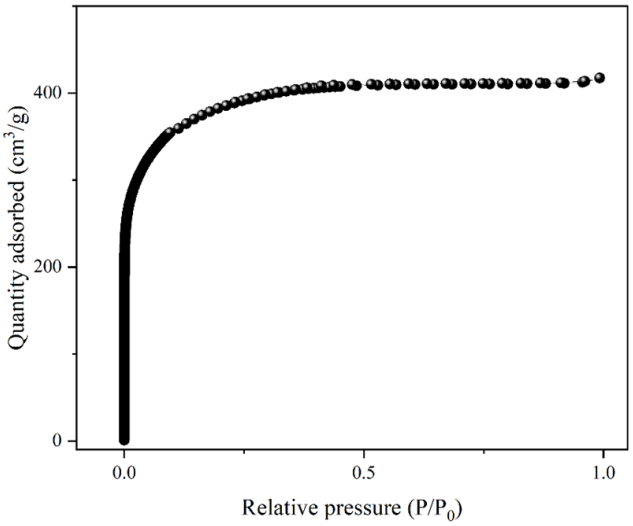

Figure S1: N_2 adsorption isotherms for AC-KOH-1:1

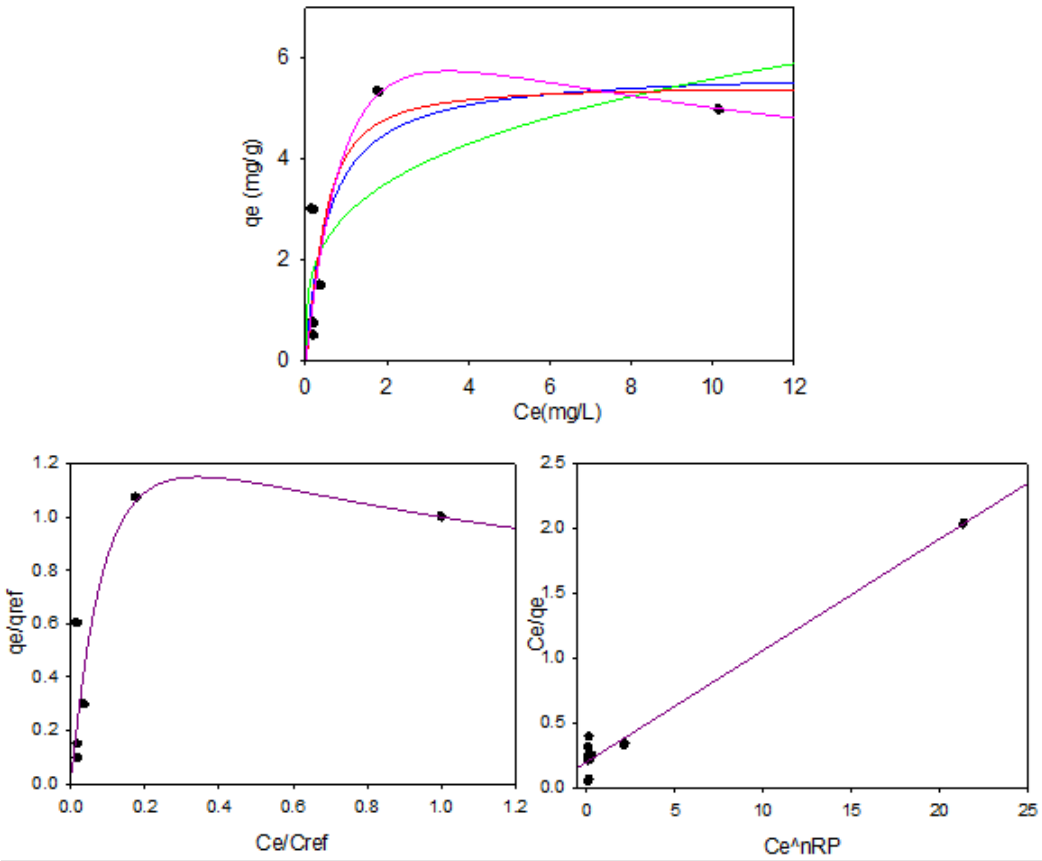

Figure S2: Adsorption isotherms for free glycerin: (A) Fitting of the Langmuir isotherm (——), Freundlich isotherm (——), and the combined Freundlich–Langmuir isotherm (——) and nonlinear regression for Redlich–Peterson (——) as expressed in equation 6. (B) Nonlinear regression for the R–P model (——) as expressed in equation 7. The regression fit for the linear form of the R–P isotherm, as expressed in equation 8 (——), is shown in (C).